

LECTURE 1

SOLID INTERIORS OF NEUTRON STARS
AND GRAVITATIONAL RADIATION

P. Haensel

*N. Copernicus Astronomical Center
Polish Academy of Sciences
ul. Bartycka 18, 00-716 Warszawa
Poland*

*to be published in "Astrophysical Sources of Gravitational Radiation"
Les Houches 1995, eds. J.-A. Marck and J.-P. Lasota*

1. INTRODUCTION

Neutron stars are the densest stable stellar objects in the present day Universe. For the typical masses $M \sim 1 - 2 M_{\odot}$, they are expected to have radii $R \sim 10$ km, so that their mean density $\bar{\rho} \sim 10^{15} \text{ g cm}^{-3}$, significantly higher than the normal nuclear density, $\rho_0 = 2.5 \times 10^{14} \text{ g cm}^{-3}$, characteristic of interiors of heavy atomic nuclei. Neutron stars are formed as very hot objects, as an outcome of gravitational collapse of massive stellar cores at the endpoint of their thermonuclear evolution, or - under specific conditions - in the gravitational collapse of mass accreting white dwarfs. Newly born neutron stars are very hot, with $T_{\text{initial}} \sim 10^{11}$ K (which corresponds to $k_{\text{B}}T \sim 10$ MeV). They cool rapidly due to neutrino emission from their interiors, so that after one year their internal temperature falls below 10^9 K. At such temperatures, matter in the neutron star interior is strongly degenerate (due to its huge density), so that the effects of temperature on the structure of neutron star, older than one year, can be neglected. Neutron stars are observed as radio pulsars, X-ray pulsars, and as X-ray bursters. Since they contain matter of the density ranging from

a few g cm^{-3} in the atmosphere to $\gtrsim 10^{15} \text{ g cm}^{-3}$ at the center, they should be considered as ‘cosmic laboratories’ for superdense matter. Observations of neutron stars yield constraints on the theory of dense matter which was used for constructing neutron star models (an introduction to physics and astrophysics of neutron stars can be found in [1])

Neutron stars are massive ($M \sim 1 - 2 M_{\odot}$), compact ($2GM/Rc^2 \sim 0.3$), and rapidly rotating (period of rotation $P \sim 1 \text{ ms}$ for millisecond pulsars) - and therefore they can be considered as potentially promising sources of continuous gravitational radiation. The shortest observed period of rotation (for radio pulsar PSR 1937+21) $P = 1.56 \text{ ms}$, which corresponds, for $R = 10 \text{ km}$, to the equatorial velocity $v_{\text{equator}} \sim 0.1c$. The expected typical moment of inertia of neutron star is $I \sim 10^{45} \text{ g cm}^2$. Crucial for the emission of continuous gravitational radiation is the time dependence (in the laboratory frame) of the quadrupole moment tensor, Q_{ij} , of the stellar mass distribution. Let us denote the amplitude of the time dependent part of Q_{ij} by $I\epsilon_{\text{eff}}$, where ϵ_{eff} describes the deviations from the axial symmetry (with respect to the rotation axis), and is usually referred to as *effective tri-axiality* of neutron star [1]. The mean power of the gravitational radiation, emitted by rotating neutron star with non-vanishing ϵ_{eff} , is proportional to ϵ_{eff}^2 , and strongly increases with rotation frequency, $\dot{E}_{\text{GR}} \propto I^2 \epsilon_{\text{eff}}^2 P^{-6}$ [1].

The non-vanishing value of ϵ_{eff} appears only under specific conditions. It can be sustained due to a partially solid nature of neutron star (a completely fluid, stably rotating body is symmetric with respect to rotation axis). As discussed in Sections 6 - 8, the existence of the solid interiors of neutron stars can lead to a non-zero ϵ_{eff} in two cases: first, due to the appearance of genuine tri-axiality, resulting from the presence of ‘mountains’ on the neutron star crust, or due to the neutron star precession. Two other possibilities, not related to the solid nature of neutron stars, and therefore not discussed in these lectures, should be mentioned. The first possibility corresponds to strong magnetic field, with symmetry axis different from the rotation axis. However, such magnetic field should be extremely strong ($B \gtrsim 10^{16} \text{ G}$), and should have quite special spatial structure to maximize ϵ_{eff} (see the lecture of S. Bonazzola and E. Gourgoulhon in this volume). The second possibility, valid also for a completely fluid star, is connected with appearance of non-axisymmetric, gravitational radiation reaction driven instabilities, [2] (see also the lecture of R. Wagoner in this volume), or with the shape instabilities, discussed in this volume in the lecture of S. Bonazzola and E. Gourgoulhon. However, both gravitational radiation reaction and shape instabilities are expected for a rotation frequency $\Omega = 2\pi/P$ close to the mass-shedding limit, $\Omega \simeq \Omega_{\text{MS}}$, while observed Ω 's are significantly lower than Ω_{MS} .

An additional attractive feature of a (partially) solid neutron star with non-zero ϵ_{eff} is connected with the remarkable stability of pulsar rotation. This could allow for long integration times (years) of periodic gravitational radiation signal from a pulsar with non-zero ϵ_{eff} .

The existence of a *solid crust* of neutron star is well established on the theo-

retical ground. Theory predicts the solid character of dense, cool (degenerate) matter for the density below $\rho_h \simeq 10^{14} \text{ g cm}^{-3}$. The existence of the solid crust is confirmed in a rather convincing way by the observations of glitches in the pulsar timing [1]. On the contrary, the possibility of existence of the *solid cores* of neutron stars, with density $\sim 10^{15} \text{ g cm}^{-3}$, is based on rather exotic models of superdense matter, and should be considered as interesting but very uncertain.

2. FORMATION AND COMPOSITION OF THE SOLID CRUST

In the present section we will restrict ourselves to the outer layer of the neutron star crust, with density up to a few times $10^{13} \text{ g cm}^{-3}$. In this density regime, the volume occupied by the atomic nuclei constitutes a small fraction of the total volume and atomic nuclei, present in the matter, can be treated as spherical. The properties of the bottom layers of the crust, with $\rho \simeq 10^{14} \text{ g cm}^{-3}$, within which the assumption of sphericity of nuclei may break down, will be discussed in Section 3.

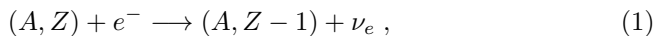
2.1. Formation of the crust: high temperature scenario

The initial temperature of the interior of neutron star formed in gravitational collapse is $T_{\text{initial}} \sim 10^{11} \text{ K}$, which corresponds to the typical energy of thermal motion of matter constituents $k_B T \sim 10 \text{ MeV}$. At such temperature matter is a multicomponent plasma of atomic nuclei (A, Z), alpha particles α , neutrons n , protons p , and electrons and positrons e^- , e^+ . The baryon density of matter (number of baryons - in our cases nucleons - in a unit volume) is given by $n_b = n_n + n_p + 4n_\alpha + n_A A$, where n_i is the number density of a species ‘i’, and where we assumed, for simplicity, that only one heavy nuclid (A, Z) is present in the matter (this is a rather good approximation, see [3]). Charge neutrality of matter requires that $n_p + n_{e^+} + 2n_\alpha + Z n_A = n_{e^-}$. Under the conditions prevailing in the interior of a newly born neutron star, matter can be assumed to be in complete nuclear equilibrium (the rate of all reactions is much higher than the rate of evolution of neutron star interior). At given n_b and T , the composition of matter is obtained from the minimization of the free energy density $f = e - Ts$, where e is the internal energy density, and s is entropy per unit volume. Neutron star cools rapidly, due to neutrino losses, and after one year internal temperature is less than 10^9 K . A standard assumption is, that during the cooling process matter was always close to the state of nuclear equilibrium, with composition always given by the minimum of f . However, at $T < 10^9 \text{ K}$ thermal contribution to f is negligible (for $\rho > 10^6 \text{ g cm}^{-3}$), and the $T = 0$ approximation (ground state of matter) is excellent. The composition of matter can be then calculated from the requirement $e = \text{minimum}$, at fixed n_b , and under the condition of charge neutrality. Such a procedure of determining the *ground state* of dense matter enables one to calculate the composition and

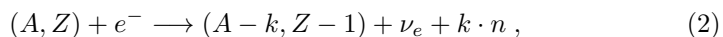
equation of state of the outer envelope of neutron star, formed from the initial, very hot state. The ground state of matter turns out to be a body-centered-cubic (bcc) lattice of nuclei (A, Z) , immersed in the uniform background of electrons. The neutron fraction in nuclei, N/Z , increases with density, and above *neutron drip* density, $\rho_{\text{ND}} = 4 - 6 \times 10^{11} \text{ g cm}^{-3}$, some of neutrons form a gas outside nuclei, so that for $\rho > \rho_{\text{ND}}$ ground state of matter is a bcc crystal of nuclei, embedded in a neutron gas, and permeated by a uniform background of electron gas.

2.2. Formation of the crust: low temperature scenario

Many neutron stars are (or were in the past) members of close binary systems, in which the second member is (was) an evolved, large radius (and therefore low surface gravity) star. Due to its huge gravitational field, neutron star accretes matter from its companion. Accretion of matter increases the mass of neutron star, leads to formation of a new outer mantle, and influences the temperature distribution within the neutron star interior. After the quasi-stationary thermal state of the neutron star interior has been reached, the internal temperature profile can be obtained from the balance of energy gains and losses. The energy gains are due to heating by infalling matter and to work done by gravitational forces compressing the stellar interior. The heat loss is due to photon emission from the neutron star photosphere and neutrino losses from the neutron star interior. The calculations, based on realistic neutron star models, lead to conclusion, that for typical accretion rates in close binary systems, $10^{-11} M_{\odot}/\text{y} < \dot{M} < 10^{-9} M_{\odot}/\text{y}$, internal temperature is always lower than 10^9 K [4, 5, 6]. At such temperatures the assumption of full thermodynamic equilibrium during the formation of the new neutron star crust is not valid: the energy of thermal motion of nuclei, $E_{\text{therm}} = \frac{3}{2}k_{\text{B}}T$, is so low compared to typical Coulomb barriers, E_{Coul} , that nuclear reactions involving charged particles are practically suppressed (blocked) (on the timescale of the neutron star evolution). The pressure and density in a given shell of the crust of accreting neutron star increase, as the accretion proceeds. The local value of electron chemical potential (Fermi energy) increases according to $\mu_e \propto (\rho Z/A)^{1/3}$, for $\rho > 10^7 \text{ g cm}^{-3}$. However, the composition of the matter can change only via those reactions between matter constituents, which are energetically possible under prevailing low temperature conditions. The only reactions, which can proceed under conditions prevailing in the neutron star crust are thus: *electron capture* on nuclei,



neutron emission (if triggered by electron captures),



as well as neutron absorption, and *pycnonuclear fusion* of neighbouring nuclei, resulting from quantum tunnelling of the Coulomb barrier due to quantum

zero-point motion around the crystal lattice sites,

$$(A, Z) + (A, Z) \longrightarrow (2A - k, Z) + k \cdot n . \quad (3)$$

The pycnonuclear regime of fusion (Greek *pycnos* - means dense) is to be contrasted with thermonuclear one; the kinetic energy of nuclei results there from the quantum effect of localization, which at sufficiently high density dominates over the thermal one: $E_{\text{zero point}} \gg E_{\text{thermal}}$. The value of $E_{\text{zero point}}$ increases with increasing density, which results in a strong density dependence of the rate of pycnonuclear fusion [1].

The crust of an accreting neutron star has a characteristic, time dependent layer structure. Let us assume, that during time t the accretion of matter onto the neutron star surface took place at constant rate \dot{M} . After time t , the outer layer of neutron star of mass $\Delta M = M_{\text{accr}} = \dot{M}t$ has thus been replaced by the accreted matter. This new shell of mass ΔM compresses the ‘old’ crust, laying below it. Each layer of the ‘old crust’ undergoes compression, characterized by the compression factor, equal to the ratio of its actual density, ρ (at time t), to its initial, original density, ρ_i (before accretion). Let us characterize the original (initial) position of the crust layer by the mass of the layers laying above it, ΔM_i , and let us denote the corresponding compression factor by $C(\Delta M_i) = \rho/\rho_i$. Notice, that the pressure at the bottom of the layer is proportional to the mass laying above it. Consider the case of $M_{\text{accr}} = 5 \times 10^{-4} M_{\odot}$, which corresponds to $t = 5 \times 10^6$ y at accretion rate $\dot{M} = 10^{-10} M_{\odot}/\text{y}$. In what follows, we will quote values obtained for a specific model of neutron star, of mass $1.4 M_{\odot}$, with liquid core ($\rho > \rho_h$) calculated for the BJI equation of state [8]. For a layer, laying originally at the neutron star surface (for this layer $\Delta M_i = 0$), one gets then $C = 10^{13}$: the density of this layer after accretion of ΔM_{accr} is $\sim 10^{13} \text{ g cm}^{-3}$. However, due to huge pressure gradient in the surface layers, the value of C decreases rapidly with increasing ΔM_i . We get $C(\Delta M_i = 5 \times 10^{-4} M_{\odot}) \simeq 2$ (i.e., the density of this layer increase from $10^{13} \text{ g cm}^{-3}$ to $2 \times 10^{13} \text{ g cm}^{-3}$). Finally, we get $C(\Delta M_i = 10^{-3} M_{\odot}) \simeq 1$. The compression of the deeper layers of neutron star crust can be neglected, and so their composition coincides with the original one.

Let us summarize our results. If neutron star accreted M_{accr} , then the composition of its outer layer of mass M_{accr} may be expected to deviate widely from the original (ground state) one: this layer of neutron star crust was formed under conditions differing strongly from the ‘high temperature’ scenario, described in the preceding section. Its actual composition can be obtained by following the evolution of matter, which was originally a hydrogen rich plasma lost by the neutron star companion. Such a program was fulfilled in [7, 8]. The differences with respect to the ground state decrease gradually with increasing density, and for the crust layers laying below the outer envelope of the mass $2M_{\text{accr}}$ the approximation of the ground state composition is very good.

2.3. Composition of the crust, melting temperature

Composition of the crust is important for determining its physical properties, such as melting temperature, elastic parameters, and thermal and electrical conductivity. Within standard approximation, the composition of neutron star crust will be determined by giving the values of A and Z of the nuclid present in the matter and, above the neutron drip point, also the mass fraction contained in the neutron gas outside nuclei, X_n . These parameters, for the ground state of the crust, and for the case of accreted crust, are shown in Figs. 1, 2. As we see from Fig. 1, the values of Z and A in accreted crust are significantly smaller, than those characteristic of the ground state of matter. The differences increase with increasing density, and for $\rho > 10^{11} \text{ g cm}^{-3}$, Z and A in the accreted crust are 2-3 times smaller than the ground state one. As seen from Fig. 2, neutron drip in an accreted crust occurs at a somewhat higher density, than in the case of the ground state of dense matter, but the values of X_n at higher densities are not dramatically different. In both cases, matter undergoes *neutronization*: the proton mass fraction decreases as the density increases.

One notices characteristic features of the density dependence of A and Z , represented in Fig. 1. They can be understood in terms of the general properties of nuclei. Only even-even nuclei (even numbers of neutrons and protons) are present - which results from the action of the pairing forces between nucleons. In the case of the ground state of dense matter, strong shell effects are clearly seen: this results from the fact, that closed-shells nuclei are particularly strongly bound. For density below 10^9 g cm^{-3} , increasingly neutron rich Ni isotopes are present, with $Z = 28$ (closed proton shell). Then, up to the neutron drip point, nuclids with closed neutron shells $N = 50$ and $N = 82$ are present in the ground state of matter. Finally, above neutron drip, closed $Z = 40$ proton subshell and $Z = 50$ proton shell are persistent, while neutron shell effects are no longer visible (which is due to the presence of the outer, unbound neutron gas). Let us notice, that up to the density $\rho \simeq 10^{11} \text{ g cm}^{-3}$ the composition of the ground state of matter is determined by the experimental data [9] ! In the case of accreted matter, one starts with ^{56}Fe shell (produced from the electron captures on ^{56}Ni , obtained at the considered accretion rate by the explosive burning of helium formed by steady burning of accreted, originally hydrogen rich plasma). Then one has to follow the evolution of this shell during low temperature compression up to $\sim 10^{13} \text{ g cm}^{-3}$ [8].

Up to now, we neglected the effect of finite temperature of neutron star crust. While at $T < 10^9 \text{ K}$ the effect of T on the composition of matter is negligible, the value of T decides whether, at a given density, dense plasma is in the liquid or solid (crystal) phase. Crystallization of the plasma is due to Coulomb forces between its constituents, which lead to localization of ions (nuclei). The importance of Coulomb energy, as compared to thermal energy of nuclei, is measured by the Coulomb coupling parameter,

$$\Gamma = \frac{Ze^2}{ak_{\text{B}}T}, \quad (4)$$

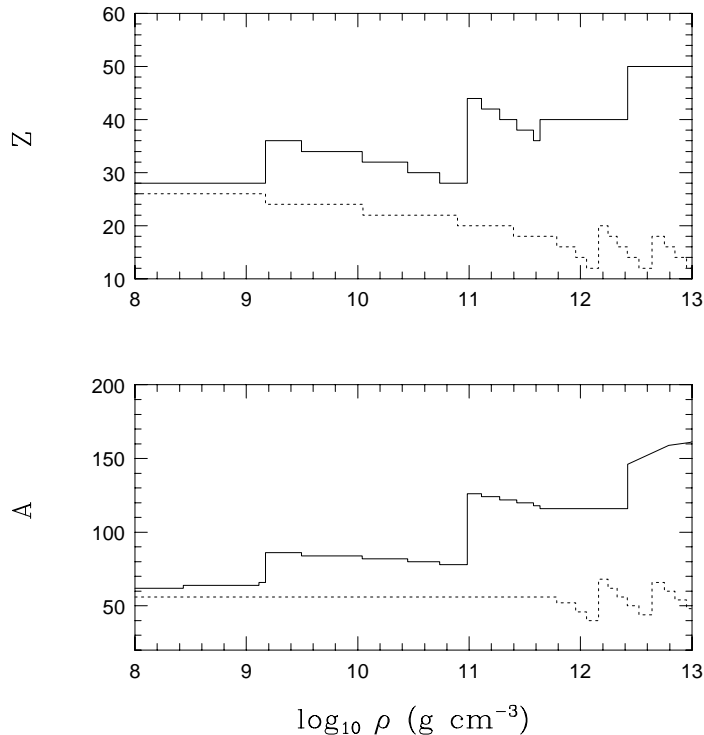


Fig. 1. — The values of Z (upper panel) and A (lower panel) for the nuclids present in dense matter for the ground state (solid line: based on [5] below neutron drip point and [4] above neutron drip) and for the accreted crust (dashed line: based on [6]).

where a is the radius of the sphere of the volume ‘per one nucleus’, $1/n_A$ (volume of the Wigner-Seitz (W-S) cell, V_{cell} ⁽¹⁾). The many-body calculations of the thermodynamic properties of dense one-component plasma show that, at fixed composition, solid phase of the plasma (bcc crystal) is energetically preferred over the liquid one for $\Gamma > \Gamma_m \simeq 178$ [11]. This corresponds to the melting temperature

$$T_m = 1.32 \times 10^6 Z^2 \left(\frac{\rho_9}{A_{\text{cell}}} \right)^{\frac{1}{3}} \text{ K}, \quad (5)$$

where A_{cell} is the number of nucleons in the Wigner-Seitz cell, and $\rho_9 =$

⁽¹⁾ The Wigner-Seitz cell is a useful object in the plasma physics; in our approximation it is a sphere containing one nucleus and Z electrons, to be electrically neutral. To a very good approximation, the energy of a plasma is a sum of energies of Wigner-Seitz cells.

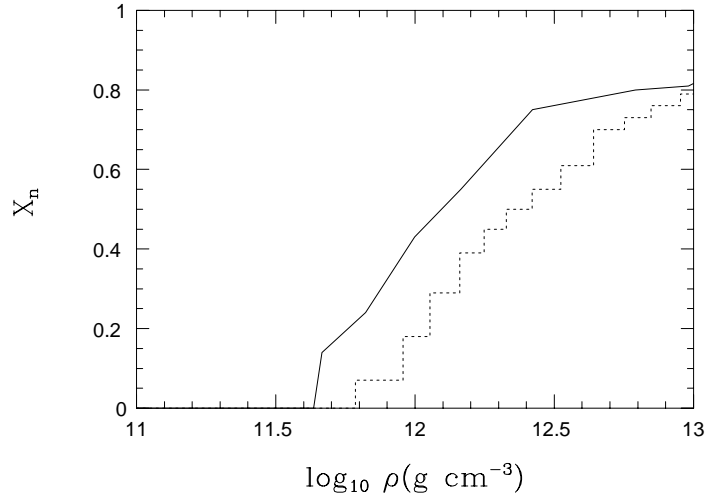


Fig. 2. — Mass fraction contained in the neutron gas outside nuclei, X_n , for the ground state of dense matter (solid line) and accreted crust (dotted line)

$\rho/(10^9 \text{ g cm}^{-3})$. For $\rho < \rho_{\text{ND}}$, we have $A_{\text{cell}} = A$, while for $\rho > \rho_{\text{ND}}$ the total number of nucleons in the W-S cell is $A_{\text{cell}} = A + n_n V_{\text{cell}}$.

The melting curve $T = T_m(\rho)$ separates the liquid and solid regions in the density - temperature plane. The melting curves for the ground state of dense matter, and for the accreted crust, are shown in Fig. 3. The difference between the two melting curves are significant for $\rho > 10^9 \text{ g cm}^{-3}$, and above neutron drip point $T_m(\text{ground state}) \gg T_m(\text{accreted crust})$. This reflects strong Z -dependence of melting temperature, combined with rather weak dependence on A_{cell} and ρ .

3. THE BOTTOM LAYERS OF THE CRUST: EXOTIC NUCLEAR SHAPES AND TOPOLOGIES

For $\rho > \rho_{\text{ND}}$ nuclei can be considered as droplets of ‘nuclear matter’, of nearly constant density $\rho_{\text{drop}} \simeq \rho_0 = 2.5 \times 10^{14} \text{ g cm}^{-3}$, immersed in a less dense neutron gas. So, above neutron drip density, nucleons are present in two coexisting phases: gaseous (neutron gas, or G-phase) and liquid (nuclear matter, or L-phase). As long as the fraction of the volume occupied by nuclei is a small fraction of the total volume of the system, droplets of nuclear matter can be treated as spherical - such a shape minimizes the surface energy of the droplets. At $T = 0$, the energy density at a given baryon density n_b can be decomposed

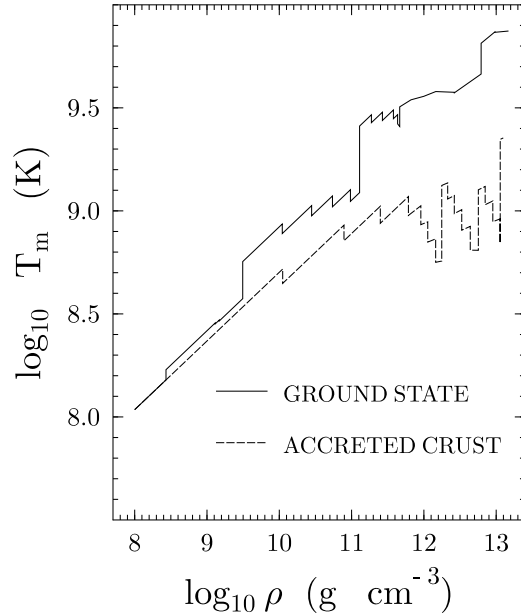


Fig. 3. — Melting temperature versus density, for the ground state composition of dense matter (solid line) and for the accreted crust (dashed line)

as

$$e(n_b, \text{parameters}) = e_{\text{vol},A} + e_{\text{surf}} + e_{\text{Coul}} + e_e + e_n, \quad (6)$$

where $e_{\text{vol},A}$ is the bulk (volume) part of the contribution from nuclei (droplets), e_{surf} is the contribution, resulting from the existence of the interface between the neutron gas and nuclear matter (surface energy), and e_{Coul} is the contribution from Coulomb interactions of charged constituents of matter. Finally, e_e is the energy density of electron gas, which permeates both phases of nucleonic matter, and e_n is the contribution of neutron gas outside nuclei (droplets). The description of nuclei embedded in neutron gas is usually done using *compressible liquid drop model* of atomic nuclei. Within this model, the problem of determination of the ground state of matter at some fixed n_b is reduced to minimization of $e(n_b, \text{parameters})$ with respect to all parameters, under the condition of charge neutrality. Let us notice, that the parameters of ‘droplets’ are modified with respect to the zero pressure case (characteristic of terrestrial nuclei) due to pressure exerted by neutron gas (which results in compression of nuclei); the presence of neutron gas influences also the surface energy term in Eq. (6).

The fraction of volume occupied by the denser L-phase increases with matter density: however, even at $\rho = 10^{13}$ g cm $^{-3}$ we have $V_L/V = 2 \times 10^{-2}$ [10], and the approximation of spherical nuclei can be expected to be valid. The situation changes, however, when we consider matter of the density close to ρ_0 , where V_L constitutes a sizable fraction of V : then, the spherical droplets may no longer minimize the energy density of the system. Such a possibility was considered long time ago by Baym, Bethe and Pethick [12], who showed that at $V_L/V = 1/2$ nuclei turn ‘inside out’, and at higher V_L/V spherical bubbles of neutron gas in nuclear matter are energetically preferred.

The problem of actual nuclear shapes for $\rho_0/3 < \rho < \rho_0$ was recently reconsidered by Lorentz et al. [13]. Using the compressible liquid drop model, these authors optimized the value of $e(n_b, \text{parameters, shape})$ with respect to the *shape* of the interface between the L and G-phase. The shapes they considered were: in three dimensions (3-D) - spherical droplets of L-phase in homogeneous G-phase, and spherical bubbles of G-phase in homogeneous L-phase; in 2-D - cylindrical rods of L-phase in homogeneous G-phase, and cylindrical tubes filled with G-phase in homogeneous L-phase. Finally, considered 1-D shapes were alternating plates of G and L-phases. The sequence of (first-order) phase transitions, obtained in [13] for a specific compressible liquid drop model of nuclei, starts at $\rho = 1.06 \times 10^{14}$ g cm $^{-3}$, where $V_L = 0.09$, $X_n = 0.76$ and $X_p = 0.03$, by a transition to ‘rods’. Then, with increasing density, transitions from ‘rods’ to ‘plates’, from ‘plates’ to ‘tubes’, and from ‘tubes’ to ‘bubbles’ take place. Finally, at $\rho_h = 1.6 \times 10^{14}$ g cm $^{-3}$ matter becomes a homogeneous mixture of neutrons, protons and electrons ($V_L = V$, $X_p = 0.03$, $X_n = 0.97$). The value of ρ_h corresponds to the bottom of the solid crust as determined in [13]. This value depends somewhat on the assumed parameters of the compressible liquid drop model, used for the description of the the L-phase, and on the $n - n$ interaction model, relevant for the description of the G-phase.

4. CRUST CONTRIBUTIONS TO STELLAR MASS AND MOMENT OF INERTIA

In order to calculate the contribution of neutron star crust to neutron star parameters, such as mass and moment of inertia, let us consider the equation of hydrostatic equilibrium for a non-rotating neutron star,

$$\begin{aligned} \frac{dp}{dr} &= -\frac{Gm\rho}{r^2} \left(1 + \frac{4\pi r^3 p}{mc^2}\right) \left(1 + \frac{p}{\rho c^2}\right) \Lambda, \\ \frac{dm}{dr} &= 4\pi r^2 \rho, \quad \Lambda = \left(1 - \frac{2Gm}{rc^2}\right)^{-1}. \end{aligned} \quad (7)$$

For sufficiently massive neutron star ($M \gtrsim 1.2 M_\odot$), the crust is thin, and contains only a small fraction of the mass of neutron star. For a shell at radius r within the crust, both $(R - r)/R$ and $(M - m)/M$ are typically few times

10^{-2} . Moreover, pressure within the crust is small compared to energy density, $p/\rho c^2 < 10^{-2}$. All these conditions enable us to rewrite Eq.(7) within the crust in the approximate form,

$$\frac{dp}{dr} = -\frac{GM\rho\Lambda(r)}{r^2}, \quad \frac{dm}{dr} = 4\pi r^2\rho, \quad (8)$$

which can be rewritten, with our approximation, as

$$\frac{dp}{dm} = -\frac{GM\rho\Lambda(R)}{4\pi R^2}. \quad (9)$$

Integration of the above equation implies, that the mass of the layer of the crust is proportional to the pressure at its bottom,

$$\Delta M(p_{\text{bot}}) \simeq \frac{4\pi R^4}{GM\Lambda(R)} p_{\text{bot}}. \quad (10)$$

Similar approximations, applied to the moment of inertia for slow, rigid rotation, lead to the formula [13]

$$\Delta I(p_{\text{bot}}) \simeq \frac{2}{3}\Delta M(p_{\text{bot}})R^2 \left(1 - \frac{2GI}{R^3c^2}\right) \Lambda(R), \quad (11)$$

where I is the total moment of inertia of the star.

Combining these equations with equation of state for the crust, one can see that the innermost layer of the crust, containing ‘exotic nuclei’, discussed in the preceding section, yields as much as half of the total crust contributions to M and I ! For a $1.4 M_{\odot}$ neutron star, I_{crust} and M_{crust} constitute $\sim 1\%$ of I and M , respectively (this agrees well with exact results reported in [13]). Both M_{crust}/M and I_{crust}/I decrease with increasing M .

The value of ρ_{h} , quoted in this lecture, deserves an additional comment. Before the appearance of the Lorentz et al. paper [13], the commonly accepted value of ρ_{h} , based on an old calculation of Baym et al. [12], was some 50% higher. Consequently, the present results for I_{crust} and M_{crust} are about two times smaller, than those obtained using the ‘old’ value of ρ_{h} [13].

5. SOLID CORES

The appearance of crystal structure for $\rho < \rho_{\text{h}}$ is due to electromagnetic (Coulomb) interactions. Possible existence of *solid cores* in the liquid interior of neutron stars would be due to specific features of the *strong interactions* between nucleons. At supranuclear density, localization of nucleons, characteristic of solid neutron star cores, discussed in [15, 16, 17, 18, 21, 22], results in the increase of the mean kinetic energy, Δe_{kin} . In order to make the crystal structure energetically preferred over the liquid one, the gain in the potential energy, Δe_{pot} , should more than compensate the increase of kinetic energy:

$\Delta e_{\text{pot}} < -\Delta e_{\text{kin}}$. Calculations were based on variational approach: for an assumed nuclear hamiltonian, the structure of the ground state is usually determined from $e(n_b, \text{parameters}) = \text{minimum}$. Transition from liquid to solid takes place, if minimization on the crystalline (periodic) structure yields lower e than that obtained for homogeneous liquid.

The possibility of solidification of pure neutron matter at sufficiently high density, due to strong repulsive short-range neutron-neutron interaction, was pointed out in the early 70-ties. However, subsequent calculations, based on more reliable solutions of the nuclear many-body problem, did not confirm these suggestions (see [14] for the history of the neutron solid). In the mid-seventies, several authors suggested existence of solid structures due to appearance of the neutral-pion-condensate ([15], [16], [18]). In all cases, solid structures were preferred because of the strong tensor component in the nucleon-nucleon interaction, which correlated nucleon spins with spatial directions. The specific crystalline structure depended on the assumed nucleon hamiltonian, while the spatial periodicities were simply related to the wave-length of the π^0 condensate, λ_{π^0} . In the calculation, reported in [15], the crystalline structure was a 3-D cubic lattice of nucleons, with lattice spacing $a = \frac{1}{2}\lambda_{\pi^0}$. In the paper of Takatsuka and Tamagaki [18], dealing with pure neutron matter with π^0 condensate, the energy was minimized by a ‘1-D solid’, consisting of alternating layers of neutrons, with opposite spin orientations, the distance between the layers being given by $d = \frac{1}{2}\lambda_{\pi^0}$. It is more appropriate to call such a structure a 1-D liquid crystal (detailed review of the work of the Kyoto group on the crystal-like structures in pion-condensed neutron star matter can be found in [20]). In all cases, crystallization took place at $\rho = 3 - 5\rho_0$.

A distinctly different model of solid neutron star core was proposed by Kutschera and Wójcik [21, 22]. As these authors show, for sufficiently low $X_p < 0.05$, protons may be treated as ‘impurities’ in neutron matter, and their behavior is determined by their interaction with neutrons, V_{np} . At the densities considered, V_{np} becomes more repulsive with increasing density, and this results in the decrease of neutron density around a p -impurity. For some nucleon-nucleon interactions, the crystalline structure appears at $\rho > 3 - 4 \rho_0$, with protons *localized* in the potential wells around the neutron density minima.

6. DEFORMATION, ELASTIC STRAIN AND MOUNTAINS

In contrast to the liquid phase of dense matter, the solid phase can support a non-vanishing shear and can be a site of elastic strain. We begin the present section with a brief summary of the basic concepts of the theory of elastic media. In what follows, for the sake of simplicity we will restrict ourselves to the standard, Newtonian version of the theory of elasticity [23]. A consistent general-relativistic theory of elastic media can be formulated; this was done by Carter and Quintana [24].

The state of thermodynamic equilibrium (ground state at $T = 0$, if thermal

effects are neglected) corresponds to specific distribution of (equilibrium) positions of ions within the neutron crust, $\mathbf{r} = (x_1, x_2, x_3)$. In what follows, we will neglect thermal effects. Such a state corresponds to the minimum of the energy density, $e = e_0 = \text{minimum}$, and to vanishing elastic strain. The *deformation* of an element of the crust with respect to the ground state configuration of ions implies a displacement of ions into new positions $\mathbf{r}' = \mathbf{r} + \mathbf{u}$, where $\mathbf{u} = \mathbf{u}(\mathbf{r})$ is the *displacement* vector. This is accompanied by the appearance of *elastic strain* (i.e., forces, which tend to return the system to the equilibrium state), and *deformation energy density* $\Delta e = e - e_0$. Uniform translation, corresponding to \mathbf{r} -independent displacement field \mathbf{u} does not contribute to Δe , and the real (genuine) deformation is described by the (symmetric) *strain tensor*

$$u_{ik} = \frac{1}{2} \left(\frac{\partial u_i}{\partial x_k} + \frac{\partial u_k}{\partial x_i} \right). \quad (12)$$

The non-zero elastic strain contributes to the stress tensor of matter, which for zero strain has the form $-\check{p}\delta_{ij}$, and which in the presence of elastic strain is given by

$$\sigma_{ij} = -\check{p}\delta_{ij} + \sigma_{ij}^{\text{strain}}. \quad (13)$$

In the case of an isotropic solid, which should be a reasonable approximation to the *macroscopically averaged* neutron star crust (consisting presumably of small, disordered on macroscopic scale, anisotropic domains), the elastic properties are determined by two elasticity parameters: the compression modulus K , and the shear modulus, μ . After the deformation, the volume of an element of matter changes according to $dV' = (1 + u_{jj})dV$, where summation is understood over the repeated indices. The diagonal strain tensor, $u_{ik} = a\delta_{ik}$, corresponds to pure compression. Compression term modifies the equation of state of the crust, adding an elastic contribution to the pressure \check{p} , Eq.(13). The elastic *shear* contribution to the stress tensor reads

$$\sigma_{ik}^{\text{shear}} = \mu \left(2u_{ik} - \frac{2}{3}u_{jj}\delta_{ik} \right). \quad (14)$$

In the case of $u_{jj} = 0$ we deal with a pure *shear* deformation of matter element, with $\sigma_{ik}^{\text{shear}} = 2\mu u_{ik}$. In general, elastic strain involves both compression and shear.

For a specific model of solid neutron star crust, the value of μ can be expressed as a function of matter density and composition. For a bcc lattice structure below ρ_{ND} one gets [25]

$$\mu = 0.295Z^2e^2n_A^{\frac{4}{3}} = 0.024 \left(\frac{Z}{26} \right)^{\frac{2}{3}} p_e, \quad (15)$$

where p_e is the electron pressure. For $\rho < \rho_{\text{ND}}$ we have $p \simeq p_e$, so that $\mu \ll p$. In view of the fact, that considered deformations will be small, the elastic effects can be always treated as small perturbation of a fluid (i.e. zero elastic strain)

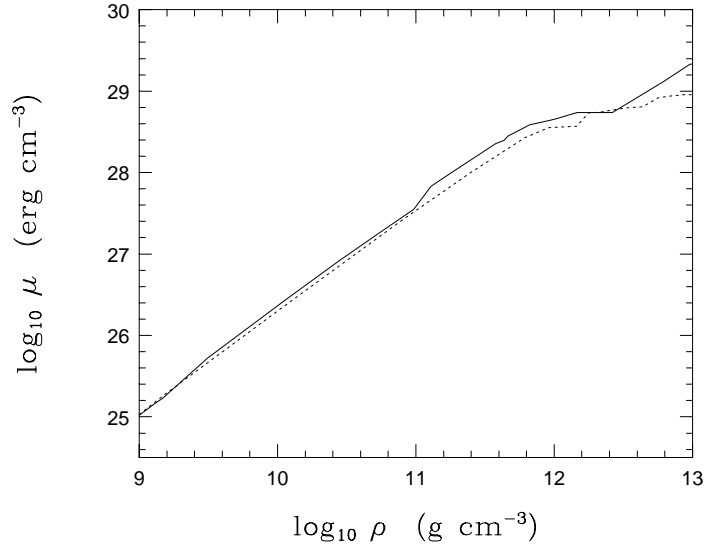


Fig. 4. — Shear modulus of neutron star crust versus density. Solid line - ground state of cold dense matter. Dotted line - accreted neutron star crust.

configuration. For $\rho > \rho_{\text{ND}}$, one has to take into account the presence of a neutron gas outside nuclei, but the inequality $|\sigma_{ij}^{\text{strain}}| \ll p$ is still valid. The shear modulus of the neutron star crust, for the ground state composition of dense matter and for the accreted crust, is plotted versus density in Fig. 4.

In the case of exotic nuclear shapes, predicted for the density interval $\frac{1}{3}\rho_0 < \rho < \rho_h$, numerical estimates of μ are not available, and in practice one is thus forced to use the extrapolation of the lower density (bcc coulomb lattice) results.

In the case of solid pion-condensed core, shear modulus has been estimated in [28], [19]. In both cases one gets an estimate $\mu_{\text{core}} \sim 10^{-2} - 10^{-1} p$, so that the elastic stresses of a hypothetical pion-condensed solid core could contribute significantly to the total stress tensor of dense matter. Actually, the perfect solid structure considered in [19] had a one-dimensional character (alternating layers); however, the macroscopically averaged core should be expected to behave as an isotropic solid. In the case of bcc lattice of localized protons, considered in [22], we expect that $\mu_{\text{core}} \ll p$, because of the small proton fraction in dense matter (the smallness of proton fraction was actually necessary for proton localization).

The presence of elastic strain modifies the equation of mechanical equilibrium of neutron star. The equation of mechanical equilibrium of an element of

neutron star reads, for Newtonian gravitation,

$$\frac{\partial \sigma_{ij}^{\text{shear}}}{\partial x_j} + \rho g_i - \frac{\partial p}{\partial x_i} = 0, \quad (16)$$

where g_i is the local value of gravitational acceleration. The presence of $\sigma_{ij}^{\text{shear}}$ allows for the permanent deformations of the neutron star crust. These deformations, supported by elastic stress, can lead to *non-sphericity* of non-rotating neutron star, and *non-axiality* of rotating neutron star. Such deformations - expected to be small (see below) - bear some resemblance to ‘mountains’ on surfaces of solid planets. The upper bound on the height of the ‘mountains’ on the neutron star crust will be discussed in the final part of this section.

Another interesting possibility, stemming from the partially solid structure of neutron star, is that of *precession*. Precession is possible in the case of the non-equal principal moments of inertia, e.g., when $I_{xx} = I_{yy} \neq I_{zz}$. Precession of partially solid neutron stars, which produces a non-vanishing value of effective tri-axiality parameter, ϵ_{eff} , will be discussed in the subsequent section.

Up to now, we restricted ourselves to Newtonian theory of elasticity. General relativistic theory of elasticity has been formulated in [24]. In its version suitable for application to isotropic solids, relativistic theory involves two material parameters K and μ - which in the limiting case of weak gravity coincide with their Newtonian counterparts. The theory formulated in [24] has been applied to fully relativistic description of partially solid, rotating neutron stars in [27].

‘Mountains’ on the neutron star crust could be formed as a result of the neutron star crust-quakes. Such crust-quakes are expected to be due to cracks (disruption of the crystal structure) in the crust, implied by sufficiently large stresses (exceeding the critical values that the crust can support), and arising, e.g., during the slowing down of pulsar rotation. Let us consider a partially solid neutron star, rotating uniformly at the angular frequency $\Omega = 2\pi/P$ around the z - axis, which is assumed to be a principal axis of the moment of inertia tensor. Let us characterize the deformation of the neutron star by the asymmetry in the principal moments of inertia, $(I_{xx} - I_{yy})/I = \epsilon$, where $I = I_{zz}$. Such a rotating, non-axisymmetric neutron star, will be a source of pulsating gravitational radiation, of angular frequency $\Omega_{\text{GR}} = 2\Omega$. The mean power of gravitational waves can be calculated using the formula derived in Section 16.6 of [1],

$$\dot{E}_{\text{GR}} = \frac{32}{5} \frac{G}{c^5} I^2 \epsilon^2 \Omega^6. \quad (17)$$

This formula can be used in order to confront the hypothesis of non-vanishing ϵ with pulsar timing. Emission of gravitational radiation implies additional loss of the kinetic energy of the pulsar, and the slowing down of its rotation, according to $\left(\dot{E}_{\text{kin}}\right)_{\text{GR}} = -\dot{E}_{\text{GR}}$. In view of the fact, that $\dot{E}_{\text{kin}} = I\Omega\dot{\Omega}$, this implies corresponding contribution to \dot{P} , which will be denoted by $(\dot{P})_{\text{GR}}$. Clearly, the slowing down, implied by gravitational radiation should be less

Table I. — Timing parameters and ϵ_{\max} for three selected radio pulsars

Pulsar:	0437-47	1957+20	Crab (0531+21)
$P(\text{ms})$	5.76	1.61	33.4
\dot{P} (10^{-19} s s $^{-1}$)	1.2	0.17	4.2×10^6
d (kpc)	0.14	1.53	2.5
ϵ_{\max}	3×10^{-8}	2×10^{-9}	1.2×10^{-3}

that the observed one, $(\dot{P})_{\text{GR}} < \dot{P}_{\text{observed}}$. This implies an observational upper bound on the value of ϵ ,

$$\epsilon < \epsilon_{\max} = 3 \times 10^{-9} \left(\frac{P}{1 \text{ ms}} \right)^{\frac{3}{2}} \left(\frac{\dot{P}}{10^{-19}} \right)^{\frac{1}{2}}, \quad (18)$$

where we assumed a ‘canonical’ value of $I = 10^{45}$ g cm². The values of ϵ_{\max} for the Crab pulsar and for two selected millisecond pulsars, together with pulsar timing parameters, are given in Table I.

The choice of pulsars in Table I deserves a comment. The Crab pulsar was chosen as a good example of a young, seismologically active pulsar (glitches observed in the Crab pulsar timing are thought to result from neutron star crust-quakes). The remaining two pulsars are the millisecond ones; short rotation periods are preferred for an efficient radiation of gravitational waves, Eq. (17). The PSR 0437-47 is very close, while PSR 1957+20 has the lowest value of \dot{P} , and the second shortest period of all observed radio pulsars: its timing yields the most stringent upper bound on ϵ .

7. SHAPE AND ENERGY OF ROTATING, PARTIALLY SOLID NEUTRON STAR

The existence of solid regions in the interior of neutron star (well established solid crust, speculative solid core) opens new possibilities for the structure and dynamics of rotating neutron stars. Partially solid neutron star can be axially non-symmetric, and can precess. In what follows, we will describe these properties of partially solid neutron stars with a simple ‘one parameter’

model of Baym and Pines [25] (hereafter referred to as BP). This model is Newtonian, and therefore enables one a very simple discussion of kinematics and energetics of rotating neutron star. Of course, neutron stars are relativistic stellar objects, with $2GM/Rc^2 \sim 0.3$, and the model of Baym and Pines is an approximation of reality. A consistent, general relativistic approach, based on the exact, relativistic theory of elasticity, was formulated by Carter and Quintana [27] (hereafter referred to as CQ). Connection between BP and CQ parameters will be discussed at the end of this section.

7.1. Liquid neutron star

Consider rigid rotation of a *liquid* neutron star around the z -axis, with angular velocity Ω . Its stationary configuration will be axially symmetric with respect to z -axis which will, at the same time, be one of the three principal axes of the moment of inertia. Due to rotation, $I_{xx} = I_{yy} < I_{zz}$. The deviation of the shape of the star with respect to the spherical one is described by the ‘oblateness parameter’

$$\epsilon = \frac{I_{zz} - \bar{I}}{\bar{I}}, \quad (19)$$

where $\bar{I} = (I_{xx} + I_{yy} + I_{zz})/3$. The total energy of the star is an even function of ϵ , and for $\epsilon \ll 1$, and at fixed total angular momentum L is given by

$$E = E_* + \frac{L^2}{2I_{zz}} + A\epsilon^2, \quad (20)$$

where E_* is the total energy of a non-rotating configuration, and where terms higher than quadratic have been neglected. Stationary configuration corresponds to $E = \text{minimum}$, at $L = I_{zz}\Omega = \text{const}$. This yields the expression for the value of oblateness parameter of a liquid star,

$$\epsilon_\Omega = \frac{\Omega^2}{4A} \left(\frac{\partial I_{zz}}{\partial \epsilon} \right)_{\Omega=0} \simeq \frac{\Omega^2 I_*}{4A}, \quad (21)$$

where I_* is the moment of inertia of a non-rotating star. For the most rapid pulsars ($P = 1.6$ ms) the typical value of ϵ_Ω is a few times 10^{-2} (assuming the mass $M \simeq 1.4 M_\odot$) [28]; the exact value of ϵ_Ω depends both on the equation of state of dense matter, and on the neutron star mass.

7.2. Rotation and elastic strain

In general case, the solid regions of rotating neutron star are a site of *elastic strain*, and in particular, they are characterized by non-vanishing shear stresses. The elastic shear contributes to the local energy density of the solid region of neutron star, with $e_{\text{shear}} = \frac{1}{2}\sigma_{ik}u_{ik} = \mu u_{ik}u_{ik}$. The contribution of shear stress to the total energy of the star is in the BP model represented by a simple expression,

$$E^{\text{shear}} = B(\zeta - \epsilon)^2. \quad (22)$$

The above formula represents a very important ingredient of the BP model. The oblateness $\check{\epsilon}$ corresponds to ‘reference relaxed configuration’ with zero shear (actually, with zero elastic strain), consisting of the same number of baryons N . This configuration will be referred to as \check{C} . The most natural assumption is that \check{C} was the configuration of neutron star just after the solidification of the crust - so that its structure coincided, to a very good approximation, with that of a fluid star. The ‘elastically relaxed’ configuration was rotating at a well defined $\check{\Omega}$. By definition, $E^{\text{shear}} = 0$ for $\Omega = \check{\Omega}$.

The one-parameter formula of the BP model, which includes the effect of elastic shear on the rotating configuration, reads

$$E = E_* + \frac{L^2}{2I} + A\epsilon^2 + B(\epsilon - \check{\epsilon})^2, \quad (23)$$

where by definition of configuration \check{C} ,

$$\check{\epsilon} = \frac{\check{\Omega}^2}{4A} \left(\frac{\partial I_{zz}}{\partial \epsilon} \right)_{\Omega=0}. \quad (24)$$

Stationary, rotating configuration with a fixed L corresponds to $E = \text{minimum}$. This yields the equilibrium value of ϵ ,

$$\epsilon = \frac{\Omega^2}{4(A+B)} \left(\frac{\partial I_{zz}}{\partial \epsilon} \right)_{\Omega=0} + \frac{B}{A+B} \check{\epsilon}. \quad (25)$$

All effects of elasticity enter through the parameter B , another important parameter is the oblateness of the ‘relaxed reference configuration’, $\check{\epsilon}$. Simple estimates of B for neutron star models with $M \simeq 1.4 M_\odot$ with liquid interior yield $B \sim 10^{-5} A$ [28]: the effect of elasticity of the solid crust on the dynamics of rotating neutron star can thus be treated as a small perturbation. In view of $B \ll A$ it is suitable to introduce a small dimensionless ‘rigidity’ parameter, which measures the relative importance of elastic shear: $b = B/A$. According to [28], $b_{\text{crust}} \sim 10^{-5}$. From Eq.(25), the contribution of the elastic strain to the oblateness of rotating neutron star is given by $(\epsilon)_{\text{elast}} \simeq b_{\text{crust}} \check{\epsilon}$. In the hypothetical case of a *solid core* in the pion-condensed neutron star interior, the effect is expected to be orders of magnitude larger, $b_{\text{core}} \sim 10^{-3} - 10^{-2}$ [28].

General relativistic version of one-parameter formula for partially solid, rotating neutron star was derived by Carter and Quintana [26]. Instead of making expansions in terms of the oblateness parameters ϵ , $\check{\epsilon}$, Carter and Quintana use Ω^2 and $\check{\Omega}^2$ as expansion parameters. In the slow rotation limit, the Newtonian parameters A and B are related to the relativistic parameters P_* and Z_* of ref.[26], by

$$P_* = \frac{I_*}{2(A+B)}, \quad Z_* = \frac{BI_*}{2A(A+B)}, \quad (26)$$

where I_* is the moment of inertia of a spherical, non-rotating configuration.

8. OBLATENESS AND PRECESSION

Even if originally fluid neutron star rotated around its symmetry axis, this situation might change after the star became partially solid. Let us consider rotating, partially solid neutron star. Let the instantaneous axis of rotation be defined by the unit vector \mathbf{n}_Ω . The deformation of neutron star results from the combined action of centrifugal forces and elastic stresses within the neutron star crust. Both effects can be treated as small perturbations. Let us switch-off deformation due to rotation; the resulting *static* configuration will still be deformed, due to elastic stresses within the neutron star crust. The symmetry axis of such a static but deformed ‘reference’ neutron star will be assumed to be given by the unit vector \mathbf{n}_0 . In the case of partially solid neutron star the vectors \mathbf{n}_Ω and \mathbf{n}_0 , may differ: this might result from the previous action of a torque, which tilted the symmetry axis of the solid component of the rotating body with respect to the rotation axis. Such torques, which could have acted on neutron star crust in the past, could be exerted by the neutron star magnetic field, by the tidal forces from a close companion, or by a passing-by neutron star. Tilting could also result from a series of ‘asymmetric’ crust-quakes. In the general case, the unit vectors \mathbf{n}_Ω and \mathbf{n}_0 will not be fixed in space, but will rotate around the fixed direction determined by the angular momentum vector \mathbf{L} . The rotation of \mathbf{n}_Ω around \mathbf{L} corresponds to well known *precession* of a solid body, typical for the case when the rotation axis does not coincide with any of the three principal axes of the body moment of inertia. Keeping only terms linear in oblateness parameters, we may write the inertia tensor of rotating neutron star as [31, 32]

$$I_{ij} = I_* \left[\left(1 - \frac{1}{2}\epsilon_\Omega - \frac{1}{2}b\check{\epsilon}\right)\delta_{ij} + \frac{3}{2}\epsilon_\Omega n_\Omega^i n_\Omega^j + \frac{3}{2}b\check{\epsilon} n_0^i n_0^j \right]. \quad (27)$$

The angular momentum of the star is given by $L_i = I_{ij}\Omega_j$. The three vectors \mathbf{L} , \mathbf{n}_Ω and \mathbf{n}_0 are coplanar [31].

For a completely liquid star, we would have $b = 0$, and we could take \mathbf{n}_Ω as z -axis. This would give

$$I_{ij}^{\text{liquid}} = I_* \left[\left(1 - \frac{1}{2}\epsilon_\Omega\right)\delta_{ij} + \frac{3}{2}\epsilon_\Omega \delta_{i3} \delta_{j3} \right], \quad (28)$$

which would imply

$$\begin{aligned} I_{xx}^{\text{liquid}} = I_{yy}^{\text{liquid}} &= I_* \left(1 - \frac{1}{2}\epsilon_\Omega\right), \\ I_{zz}^{\text{liquid}} &= I_* (1 + \epsilon_\Omega). \end{aligned} \quad (29)$$

In the above equations, I_* is the moment of inertia of a spherical, non-rotating neutron star.

In the linear approximation, the deformations described by the oblateness parameters ϵ_Ω and $b\check{\epsilon}$ can be treated independently. From the Euler equations,

one finds that the angular velocity vector (as calculated in the solid body reference system) precesses around the direction of \mathbf{n}_0 , with precession frequency

$$\Omega_{\text{prec}} = \frac{3}{2} b \check{\epsilon} \Omega . \quad (30)$$

The free precessional frequency of a partially solid neutron star is thus determined by internal stellar structure and distribution of internal elastic strain.

While it might appear, that the free precession of partially solid neutron stars is a rather common phenomenon, observations of radio pulsars give only one (and debatable) example of the possible presence of precession in the pulsar timing. Analysing timing data for the Crab pulsar, spanning the time interval of five years, Lyne et al. [29] find ‘quasi-sinusoidal’ deviations from the regular pulsar slow-down, with an approximate period of approximately 20 months. It should be stressed, that originally Lyne et al. preferred the interpretation of it in terms of the so called ‘Tkachenko oscillations’ of the superfluid interior of neutron star. Further quantitative considerations indicated, however, the relevance of the solid interior of neutron star for explaining the specific period of modulations [30]. Precession of the solid crust remains thus one of possible explanations [30]. Applying our precession model for explaining observed quasi-sinusoidal deviations, we would get $(b\check{\epsilon})_{\text{Crab}} \sim 10^{-10}$.

9. GRAVITATIONAL RADIATION FROM PRECESSING PULSARS

9.1. Mean power of gravitational radiation

Precession of a deformed pulsar implies radiation of gravitational waves. The mean power of gravitational radiation is calculated using the general formula,

$$\dot{E}_{\text{GR}} = \frac{1}{5} \frac{G}{c^5} \left\langle \frac{d^3 \mathcal{I}_{jk}}{dt^3} \frac{d^3 \mathcal{I}_{jk}}{dt^3} \right\rangle , \quad (31)$$

where \mathcal{I}_{ij} is traceless mass quadrupole moment in laboratory (observer’s) system [1]. In the lowest order in ϵ ’s, terms proportional to ϵ_Ω do not contribute to the relevant time derivatives, and therefore when calculating \mathcal{I}_{ij} we may put $\epsilon_\Omega = 0$. The calculation gives [1]:

$$\dot{E}_{\text{GR}} = \frac{2}{5} \frac{G}{c^5} (I_1 - I_3)_{\epsilon_\Omega=0}^2 \Omega^6 \theta^2 , \quad (32)$$

where θ is the ‘wobble angle’ (the angle between the reference (‘solid body’) symmetry axis \mathbf{n}_0 and (fixed in laboratory, inertial reference frame) direction of \mathbf{L} ; we assumed that $\theta \ll 1$. In Eq. (32), I_1 and I_2 are principal moments of inertia in the neutron star (body) reference system ($I_1 = I_{xx}$, $I_3 = I_{zz}$).

The frequency of the gravitational waves is *approximately* equal to the pulsar frequency, Ω , namely $\Omega_{\text{GR}} = \Omega + \frac{3}{2}b\check{\epsilon}\Omega$ [33, 32]. In our case, we have

$$I_1 - I_3 = \frac{3}{2}b\check{\epsilon}I_* , \quad (33)$$

so that the formula for \dot{E}_{GR} can be written in the form

$$\dot{E}_{\text{GR}} = \frac{32}{5} \frac{G}{c^5} I^2 \Omega^6 \epsilon_{\text{eff}}^2 , \quad (34)$$

where the *effective tri-axiality* is

$$\epsilon_{\text{eff}} = \frac{3}{8}b\check{\epsilon}\theta , \quad (35)$$

and $I \equiv I_*$.

9.2. Estimating b , $\check{\epsilon}$, and θ

For a neutron star of mass $M \simeq 1.4 M_\odot$ the existing estimates give $b_{\text{crust}} \sim 10^{-5}$ [28]. In the hypothetical case of a more massive neutron star with a solid pion condensed core, a very uncertain estimate is $b_{\text{core}} \sim 10^{-3} - 10^{-2}$ [28].

Let us first calculate the value of ϵ as a function of angular frequency of radio pulsar. Using Eq.(21), we get

$$\epsilon \simeq \epsilon_\Omega = 10^{-3} \left(\frac{I}{10^{45} \text{ g cm}^2} \right) \left(\frac{A}{10^{53} \text{ erg}} \right) \left(\frac{P}{10 \text{ ms}} \right)^{-2} . \quad (36)$$

Neutron star, born with some initial period of rotation, P_{init} , slows down during its life as a radio pulsar. In Table II we give numerical estimates of initial and present oblateness parameters, ϵ_{init} and ϵ for the most rapid millisecond pulsar, PSR 1937+21, and for the Crab pulsar. In both cases we assumed $I = 10^{45} \text{ g cm}^2$ and $A = 10^{53} \text{ erg}$. Initial period of the Crab pulsar was calculated using the magnetic dipole formula for pulsar slowdown [1]. In the case of the PSR 1937+21, we considered two cases. The millisecond pulsars are believed to be previously radio-dead, old pulsars ($P \sim$ seconds), revived by accretion of matter in close binary system. In the first case, we assumed that the old pulsar (predecessor of PSR 1937+21) had in the beginning of the accretion era small deformation, equal to ϵ_Ω at the beginning of this era, when $P = P_{\text{init}} = 1 \text{ s}$. We assumed additionally, that this initial configuration was elastically relaxed (no elastic strain). Notice, that in the case of the Crab pulsar the initial configuration was hot and liquid, while in the case of PSR 1937-21 the pulsar was assumed to be sufficiently old to be elastically relaxed.

In principle, in the case of PSR 1937+21, we could contemplate a rather extremal situation, when the pulsar keeps the initial oblateness from its ‘first birth’. Such a situation, which would require a very high resilience of the stellar solid, would lead to a Crab-like initial oblateness, which is indicated

Table II. — Initial and present oblateness parameters of two pulsars

Pulsar:	1937+21	Crab (0531+21)
P	1.56 ms	33 ms
P_{init}	1 s (10 ms)	17 ms
ϵ_{init}	10^{-7} (10^{-4})	3×10^{-4}
ϵ_{Ω}	4×10^{-2}	9×10^{-5}

within the brackets. Notice however, that during the accretion era the old pulsar had to accrete some $\sim 0.1 M_{\odot}$, in order to spin-up to $P \sim 1$ ms. In view of this, the ‘old crust’, with large initial oblateness, was presumably ‘molten’ by compression, and transformed into the outer layer of the liquid interior. It seems thus, that in order to keep the ‘first birth’ oblateness, the millisecond pulsar would have to contain a *solid core*.

The value of the ‘wobble angle’, θ , is limited by the critical strain, which the solid crust can support. The crust breaks down (fractures) if the shear exceeds some critical value. In terms of oblateness parameters, the condition for disruption of the solid is $|\epsilon - \check{\epsilon}| > \Theta_{\text{crit}}$, where Θ_{crit} is called ‘critical angle’ (notice that shear deformation changes angles within the crystalline structures) [32]. A non-zero wobble angle implies an elastic strain within the solid region of the star. For typical terrestrial solids, $\Theta_{\text{crit}} \sim 10^{-5} - 10^{-4}$. This would imply $\check{\epsilon} \simeq \epsilon_{\Omega}$ (a stringent condition in the case of millisecond pulsars). Such a low Θ_{crit} would limit the wobble angle to $\theta \lesssim 10^{-3}$ [32]. Let us notice, that for a *perfect Coulomb* lattice - which seems to be better suited as a model of neutron star crust - calculations give $\Theta_{\text{crit}} \sim 10^{-2} - 10^{-1}$, which would imply $\check{\epsilon} \simeq \epsilon_{\text{init}}$, and no limitations on θ ! (An interesting discussion of ‘elastic strength’ of neutron star’s crust, referring also to terrestrial experiments on ‘near Coulomb’ metallic microcrystals, can be found in [36].) However, neutron star crust should be expected to be very far from the ‘perfect crystal’ structure, and therefore we may expect a significantly lower value of Θ_{crit} . In any case, it is difficult to point out a mechanism, which could build up a wobble angle $\theta \lesssim 1$ [32].

Table III. — Timing data, oblateness, and effective tri-axiality for pulsars

Pulsar:	1937+21	1957+20	Crab(0531+21)
$P(\text{ms})$	1.56	1.61	33
\dot{P} (10^{-19} s s $^{-1}$)	1.0	0.17	4.2×10^6
ϵ_{max}	6×10^{-9}	2×10^{-9}	1.2×10^{-3}
ϵ_{Ω}	4×10^{-2}	4×10^{-2}	9×10^{-5}
ϵ_{eff} - case a	1×10^{-10}	1×10^{-10}	3×10^{-13}
ϵ_{eff} - case b	4×10^{-13}	4×10^{-13}	3×10^{-12}

10. GRAVITATIONAL RADIATION FROM PRECESSING PULSARS AND PULSAR TIMING

The slowing-down of the pulsar rotation due to gravitational radiation is limited by the measured value of \dot{P} , so that $(\dot{P})_{\text{GR}} < \dot{P}_{\text{obs}}$. This yields observational constraint on the effective tri-axiality of pulsar,

$$\begin{aligned} \epsilon_{\text{eff}} &< \epsilon_{\text{max}} = 3 \times 10^{-9} \left(\frac{P}{1 \text{ ms}} \right)^{\frac{3}{2}} \left(\frac{\dot{P}}{10^{-19}} \right)^{\frac{1}{2}}, \\ \epsilon_{\text{eff}} &= \frac{3}{8} b \check{\epsilon} \theta. \end{aligned} \quad (37)$$

We will consider two limiting cases, of a small and large critical strain, respectively. Numerical estimates for these two limiting cases, based on the timing data for two millisecond pulsars and the Crab pulsar, are given in Table III. In all cases, we assumed rigidity parameter $b = 10^{-5}$. For the scenario corresponding to ‘case a’, we use a conservative assumption of $\theta = 10^{-3}$. In view of the assumed small value of critical strain, we have in this case $\check{\epsilon} \simeq \epsilon_{\Omega}$. Due to rapid present rotation of millisecond pulsars, their effective tri-axialities are, in ‘case a’, some three orders of magnitude higher than this of the Crab pulsar. The situation changes in ‘case b’ (large critical strain). Then, we could contemplate the value of θ for millisecond pulsars, which could be as large as 1; however, due to the large critical strain, we should expect $\check{\epsilon} = \epsilon_{\text{init}}$, corresponding to $P_{\text{init}} = 1$ s, which reduces the effective tri-axiality by some three

orders of magnitude as compared to the ‘case a’. For the Crab pulsar we put $\tilde{\epsilon} = \epsilon_{\text{init}}$, but in view of its short age (941 years) we made a conservative choice of $\theta = 10^{-3}$ (no sufficient time to built a large tilt of the ‘solid body axis’ with respect to rotation axis). Under these assumptions, we get in ‘case b’ similar values of effective tri-axiality for the most rapid millisecond pulsars and the Crab pulsar.

The presence of a sufficiently large *solid core* would imply some difficulties in confrontation with pulsar timing. In such a (highly speculative) case, we would expect $b \simeq b_{\text{core}} \sim 10^{-2} - 10^{-1}$. Even with a rather small $\theta = 10^{-3}$, the large value of rigidity parameter would lead to effective tri-axiality largely exceeding the observational upper bound for millisecond pulsars. Moreover, as the critical strain for the solid core may be expected to be very large, the possible ‘wobble angle’ that could be built during star evolution could, in principle, be large. Confronting these theoretical speculations with pulsar timing leads to conclusion, that if millisecond pulsars contain a solid core, then their wobble angles are extremely small. A more restrictive statement is that millisecond pulsars are just unlikely to contain a massive solid core.

11. DETECTABILITY

The radio pulsars with a non-zero tri-axiality could be promising sources of continuous gravitational radiation. The most attractive in this respect are the nearby millisecond pulsars with $\epsilon_{\text{eff}} \sim 10^{-9}$ [34]. Consider two selected millisecond pulsars, PSR 1957+20 and PSR 0437-47. The advantage of the first one is its very short period, $P = 1.6$ ms (the distance being $d = 1530$ pc). On the other hand, the second millisecond pulsar is much closer, at $d = 140$ pc.

Millisecond pulsars with non-zero tri-axiality would be interesting sources of continuous, nearly monochromatic gravitational radiation, provided some additional conditions are satisfied. As we could see, the fact that millisecond pulsars are such precise clocks ($\dot{P} < 10^{-19}$ s s $^{-1}$!), imposes rather stringent constraints on the maximum value of ϵ_{eff} . The timing of the millisecond pulsars tells us, that the possible amplitude of the gravitational waves should be sufficiently small to be consistent with observations. As a consequence, the detectability of gravitational waves from the nearby millisecond pulsars by the forthcoming generation of the LIGO and VIRGO detectors would be possible only if the periodic signal could be integrated over the time of a few years [34]. This would require a sufficiently long lifetime of the precession or wobble.

In the approximation, in which the coupling of the solid and liquid regions of neutron star are neglected, liquid interior of neutron star cannot participate in stellar precession. However, such a coupling exists, and detectability of continuous gravitational radiation requires that the damping times connected with the liquid-solid coupling be substantially longer than a few years [32]. Finally, the ‘wobble’ is damped by the gravitational radiation itself (see Exercise 16.13 in [1]). Explicit calculation shows that the characteristic timescale

$\tau_{\text{wobble}}^{\text{GR}} \sim 10^3 (b\tilde{\epsilon}/10^{-6})^{-2} (P/1 \text{ ms})^{-4}$ years (see, e.g., [35]): the detectability requires, that $\tau_{\text{wobble}}^{\text{GR}}$ be substantially longer than a few years. Our discussion of the damping timescales indicates thus, that the situation in which a non-zero tri-axiality is due to sufficiently large, genuine ‘mountains’ on the neutron star crust, is the most attractive one. This conclusion seems to be in a surprising harmony with the location of Les Houches School, dominated by the magnificent *massif du Mont Blanc*, so admired by all of us during the coffee breaks.

Acknowledgments

I am grateful to my wife for a critical reading of the manuscript, and for helpful remarks. I am also grateful to A.D. Kaminker for preparing Figure 3, and to E. Gourgoulhon for reading of the manuscript, and for helpful comments. This work was supported in part by the KBN grant No. 2 P304 014 07.

References

- [1] Shapiro S. L., Teukolsky, S. A., *Black Holes, White Dwarfs and Neutron Stars*, (Wiley, New York, 1983).
- [2] Friedman, J. L., Ipser, J. R., *Phil. Trans. R. Soc. Lond. A* **340** (1992) 391.
- [3] Burrows, A., Lattimer, J. M., *Astrophys. J.* **285** (1984) 295.
- [4] Fujimoto, M. Y., Hanawa, T., Iben, I., Jr., Richardson, M.B., *Astrophys. J.* **278** (1984) 813.
- [5] Fujimoto, M. Y., Hanawa, T., Iben, I., Jr., Richardson, M.B., *Astrophys. J.* **315** (1987) 198.
- [6] Miralda-Escudé, J., Haensel, P., Paczyński, B., *Astrophys. J.* **362** (1990) 572.
- [7] Haensel, P., Zdunik, J. L., *Astron. Astrophys.* **227** (1990) 431.
- [8] Haensel, P., Zdunik, J. L., *Astron. Astrophys.* **229** (1990) 117.
- [9] Haensel, P., Pichon, B., *Astron. Astrophys.* **283** (1994) 313.
- [10] Negele, J. W., Vautherin, D., *Nucl. Phys. A* **207** (1973) 298.
- [11] Slattery, W. L., Doolen, G. D., DeWitt, H. E., *Phys. Rev. A* **26** (1982) 2255.
- [12] Baym, G., Bethe, H. A., Pethick, C. J., *Nucl. Phys. A* **175** (1970) 225.
- [13] Lorentz, C. P., Ravenhall, D. G., Pethick, C. J., *Phys. Rev. Lett.* **70** (1993) 379.
- [14] Baym, G., Pethick, C.J., *Ann. Rev. Nucl. Sci.* **25** (1975) 27.
- [15] Pandharipande, V.R., Smith, *Nucl. Phys. A* **237** (1976) 507.
- [16] Tamagaki, R., Takatsuka, T., *Prog. Theor. Phys.* **56** (1976) 1340.
- [17] Tamagaki, R., Takatsuka, T., *Prog. Theor. Phys.* **58** (1977) 694.
- [18] Takatsuka, T., Tamiya, K., Tatsumi, T., Tamagaki, R., *Prog. Theor. Phys.* **60** (1978) 1753.

- [19] Takatsuka, T., Tamagaki, R., *Prog. Theor. Phys.* **79** (1988) 274.
- [20] Kunihiro, T., Muto, T., Takatsuka, T., Tamagaki, T., Tatsumi, T., *Prog. Theor. Phys. Suppl.* **112** (1993) .
- [21] Kutschera, M., Wójcik, W., *Acta. Phys. Polonica* **B 21** (1990) 823.
- [22] Kutschera, M., Wójcik, W., *Nucl. Phys.* **A 581** (1995) 706.
- [23] Landau, L.D., Lifshitz, E.M., *Theory of Elasticity*, (Pergamon Press, Oxford, 1984).
- [24] Carter, B., Quintana, H., *Proc. Roy. Soc. London. Ser. A.* **331** (1972) 57.
- [25] Baym, G., Pines, D., *Ann. Phys. (N.Y.)* **66** (1971) 816.
- [26] Carter, B., Quintana, H., *Ann. Phys. (N.Y.)* **95** (1975) 74.
- [27] Carter, B., Quintana, H., *Astrophys. J.* **202** (1975) 511.
- [28] Pandharipande, V. R., Pines, D., Smith, R. A., *Astrophys. J.* **208** (1976) 550.
- [29] Lyne, A. G., Pritchard, R. S., Smith, F. G., *Mon. Not. R. Astr. Soc.* **233** (1988) 667.
- [30] Lyne, A.G., Graham-Smith, F., *Pulsar Astronomy*, (Cambridge UP, Cambridge, 1990).
- [31] Pines, D., Shaham, J., *Phys. Earth Planet. Inter.* **6** (1972) 103.
- [32] Alpar, A. M., Pines, D., *Nature* **314** (1985) 334.
- [33] Zimmerman, M., Szedenits, E. Jr., *Phys. Rev. D* **20** (1979) 351.
- [34] New, K. C. B., Chanmugan, G., Johnson, W. W., Tohline, J.E., *Astrophys. J.* **450** (1995) 757.
- [35] de Araujo, J. C. N., de Freitas Pacheco, J. A., Horvath, J. E., Cattani, M., *Mon. Not. R. Astron. Soc.* **271** (1994) L31.
- [36] Ruderman, M., in: *The Structure and Evolution of Neutron Stars*, D. Pines, R. Tamagaki, S. Tsuruta (editors) (Addison-Wesley, Redwood City, Ca., 1992) p.353.